Remote Sens. **2015**, *7*, 15224-15243; doi:10.3390/rs71115224

OPEN ACCESS

remote sensing

ISSN 2072-4292

www.mdpi.com/journal/remotesensing

Article

Analysis of the 2014 "APEC Blue" in Beijing Using More than One Decade of Satellite Observations: Lessons Learned from Radical Emission Control Measures

Ran Meng [1,†], Feng R. Zhao [2], Kang Sun [3,‡], Rui Zhang [2], Chengquan Huang [2] and Jianying Yang [4,*]

[1] Department of Geography, University of Utah, Salt Lake City, UT 84112, USA, E-Mail: mengran07@gmail.com

[2] Department of Geographical Sciences, University of Maryland, College Park, MD 20742, USA, E-Mails: fengzhao@umd.edu (F.R.Z.); zhangrui@umd.edu (R.Z.); cqhuang@umd.edu (C.H.)

[3] Department of Civil and Environmental Engineering, Princeton University, Princeton, NJ 08544, USA, E-Mail: Franksun1117@gmail.com

[4] School of Soil and Water Conservation, Beijing Forestry University, Beijing 100083, China

† Present address: Environmental and Climate Sciences Department, Brookhaven National Laboratory, Bldg. 490A, Upton, NY 11973, USA; E-Mail: ranmeng@bnl.gov.

‡ Present address: Atomic and Molecular Physics Division, Harvard-Smithsonian Center for Astrophysics, 60 Garden Street, Cambridge, MA 02138, USA; E-Mail: kang.sun@cfa.harvard.edu.

***** Author to whom correspondence should be addressed; E-Mail: yangjy07@hotmail.com.

Academic Editors: Richard Müller and Prasad S. Thenkabail

Received: 8 June 2015 / Accepted: 2 November 2015 / Published: 13 November 2015

Abstract: During the 2014 Asia-Pacific Economic Cooperation (APEC) Economic Leaders' Meetings in Beijing, the Chinese government made significant efforts to clear Beijing's sky. The emission control measures were very effective and the improved air quality during the APEC Meetings was called the "APEC Blue". To monitor and estimate how these emission control measures affected air quality in Beijing and its five neighboring large cities (Tianjin, Shijiazhuang, Tangshan, Jinan, and Qingdao), we compared and analyzed the satellite-retrieved Aerosol Optical Thickness (AOT) products of the pre-APEC (18–31 October), APEC (1–11 November), and post-APEC periods (11–31 November) in 2002–2014 and daily $PM_{2.5}$ measurements of the three periods in 2014 on the ground. Compared with the pre- and

post-APEC periods, both ground and satellite observations indicated significantly reduced aerosol loading during the 2014 APEC period in Beijing and its surroundings, but with apparent spatial heterogeneity. For example, the peak value of $PM_{2.5}$ in Beijing were around 100 $\mu g \cdot m^{-3}$ during the APEC period, however, during the pre- and post-APEC periods, the peak values were up to 290 $\mu g \cdot m^{-3}$. The following temporal correlation analysis of mean AOT values between Beijing and other five cities for the past thirteen years (2002–2014) indicated that the potential emission source regions strongly impacting air quality of Beijing were confined within central and southern Hebei as well as northern and southwestern Shandong, in correspondence with the spatial pattern of Digital Earth Model (DEM) of the study region. In addition to stringent emission control measures, back trajectory analysis indicated that the relatively favorable regional transport pattern might also have contributed to the "APEC Blue" in Beijing. These results suggest that the "APEC Blue" is a temporarily regional phenomenon; a long-term improvement of air quality in Beijing is still challenging and joint efforts of the whole region are needed.

Keywords: APEC Blue; North China Plain; emission control; aerosol optical thickness; MODIS; VIIRS; $PM_{2.5}$; public health; air pollution

1. Introduction

Air pollution episodes over China in recent years have become a top environmental and health concern for the Chinese public and government [1,2]. During the recent 2014 Asia-Pacific Economic Cooperation (APEC) Economic Leaders' Meetings in Beijing, 5–11 November 2014 (called the 2014 Beijing APEC Meetings hereafter), the Chinese government made significant efforts in air pollution control to ensure a healthful and pleasant experience for attending leaders and journalists from all over the world. Beijing and central cities in four provinces on the North China Plain employed stringent emission control measures, designed to improve air quality in Beijing during the APEC Meetings, and these measures were even more radical than those during the 2008 Beijing Olympic Games [3]. Starting on 1 November 2014 and lasting through the Meetings (11 November 2014), these emission control measures included closing thousands of coal-consuming factories around Beijing and its surroundings, imposing traffic restrictions on millions of private vehicles from driving on alternate days, banning governmental and commercial vehicles in large urban centers, closing government offices, agencies, and public schools in Beijing, and halting construction and demolition work [4–6].

These emission control measures were very effective. The dramatic improvement in air quality during the 2014 Beijing APEC Meetings is now referred to as "APEC Blue". According to the Beijing Municipal Environmental Protection Bureau (BMEPB), particulate matter, aerosol, with aerodynamic diameters less than 10 μm (PM_{10}) and less than 2.5 μm ($PM_{2.5}$) concentrations were reduced by 63% and 35% respectively, compared with the pre-APEC Meetings levels. Nitrogen oxides (NO_x) and sulfur dioxide (SO_2) concentrations were also reduced by more than 40%. NO_x and SO_2 from fossil fuel combustion are precursors to sulfate and nitrate aerosols [7,8], accounting for the majority of $PM_{2.5}$ during pollution episodes. This type of mixture has been the main source of aerosol loading over eastern

China [9]. Particulate matter, PM_{10} and $PM_{2.5}$ especially, is highly respirable and a leading global environmental risk to public health [10–12]. For example, a recent study shows that inhalation cancer risk was significantly reduced, due to the $PM_{2.5}$ emission control measures imposed during the 2008 Beijing Olympics Games [13].

Long-term air quality improvement in Beijing is a regional issue in nature, made clear by the emission control practices before and during the 2008 Beijing Olympic Games and related air quality studies [14–17]. However, studies monitoring the impact of emission control practices on short-term air quality improvement are less common. The APEC Blue event offers an excellent research opportunity to fill in this gap. Using ground-based instruments, Zhang *et al.* [18] recently found the atmospheric concentration of submicron aerosol particles (PM_1) in Beijing decreased 63% during the APEC Meetings, compared with the pre-APEC Meetings level. Yang *et al.* [19] compared the composition and sources of $PM_{2.5}$ in Beijing during the heating period of 2013 and 2014. They concluded that, as a result of emission control measures, the major components of $PM_{2.5}$ in Beijing largely decreased. Meanwhile, the contribution ratios of different major components of $PM_{2.5}$ changed significantly. The surface and near surface sources (e.g., biomass/waste burning and traffic related pollution) contributed much more to the $PM_{2.5}$ components in Beijing during the APEC Meetings, compared with the same period of 2013; in contrast, secondary aerosols (e.g., SO_2 and NO_x)—the dominant source of $PM_{2.5}$ usually in Beijing—reduced greatly as well as aerosols from long-range transport [19].

Recent ground-based studies on the APEC Blue have been informative in understanding the aerosol pollutants in Beijing, but there are several drawbacks that can be remedied via alternative measurement strategies such as satellite observations. Specifically, compared with global Chemical Transport Models (CTMs) and *in situ* observations (*i.e.*, ground-based), satellite-based analysis provide a large spatial coverage and reliable repeated measurements for monitoring aerosol loading and their transport patterns [20]. In particular, for a large geographic area (*i.e.*, North China Plain), satellite observations allow for the analysis of time series data going back to the early 2000s. Satellite-retrieved column Aerosol Optical Thickness (AOT), a unit less measure of the column integrated extinction of radiation by atmospheric particles, has been successfully related to surface aerosol loading and air quality [3,20–25]. A higher AOT value suggests higher column aerosol loading and therefore likely lower air quality [20]. Satellite-retrieved estimates of ground $PM_{2.5}$ have advanced in recent years, due to the development of advanced AOT satellite retrievals, of CTMs, and of *in situ* observations [20–22,26–29].

Huang *et al.* [3] successfully evaluated the changes in air pollutants in Beijing and surroundings during the APEC period using multiple satellite datasets, including AOT. As a result of stringent emission control measures, dramatic reductions in air pollutants were detected over the North China Plain, but with the lifting of these measures, air quality dropped during the post-APEC period [3]. They also found that areas impacting Beijing air quality shrank and were confined within Hebei, compared to the previous three years (2011–2013) [3]. However, mainly due to the limit on the spatial resolution of remote sensing datasets used (e.g., MODIS Level-3 global-gridded AOT product with a spatial resolution of 110 km, see Section 2.2), Huang *et al.* [3] analyzed the APEC Blue at a relatively coarse spatial scale (*i.e.*, province scale). As a result, the spatial heterogeneity in aerosol loading within Beijing and its surrounding provinces during the study period has not been explored deeply. This information can be valuable and informative for the long-term effort of the Chinese government in controlling air

pollution in Beijing and its surroundings [30], especially considering the recent debate on the contribution of regional transport to the aerosol pollutants in Beijing [31–33].

Using a finer spatial resolution remote sensing dataset (*i.e.*, MODIS level-2 AOT product with a spatial resolution of 10 km and VIIRS AOT product with a spatial resolution of 6 km , see Section 2.2), we explored spatial-temporal patterns of aerosol loading before, during, and after the 2014 Beijing APEC Meetings. The spatial heterogeneity in aerosol loading during these periods was investigated using both satellite-retrieved AOT and ground $PM_{2.5}$ measurements with a focus on Beijing and its five neighboring large cities (Tianjin, Shijiazhuang, Tangshan, Jinan, and Qingdao). Back trajectory and surface weather analysis were also conducted to explore the effects of regional transport pattern and local weather conditions on the aerosol loading during studying periods. At last, with more than one decade of AOT remote sensing products from 2002 to 2014, we conducted a temporal correlation analysis of mean AOT values of the APEC period in 2002–2014 between Beijing and its five neighboring cities, and the result indicated illuminating clues on the geographic extent of potential emission source regions that strongly impact air quality in Beijing.

2. Materials

2.1. Study Area

Figure 1 shows the city center locations of Beijing (population 19.61 million, National Bureau of Statistics of China (NBSC), 2012) and five big cities within several hundred kilometers of Beijing. Tianjin (12.94 million), adjacent to Beijing, is one of the five national central cities in China. Surrounding Beijing and Tianjin are two large populated and industrialized provinces—Hebei and Shandong. Shijiazhuang (10.16 million) and Jinan (6.81 million), located inland, are the capitals of Hebei and Shandong provinces, respectively. Tangshan (7.58 million) and Qingdao (8.72 million) are two large and important coastal urban centers in Hebei and Shandong provinces, respectively. Except for Qingdao, stringent emission control measures were implemented in the five other cities during the 2014 Beijing APEC Meetings. Due to the unique topography and location of Beijing, the wind direction/regional circulation pattern can strongly impact the air quality in Beijing [19,31]. Northward wind, carrying fresh air masses from the northern mountain areas, is helpful for the dispersion of aerosol pollutants, but the southward wind, carrying polluted air masses from the heavily populated North China Plain, can exacerbate the air pollution (Figure 1) [31].

2.2. Data and Analysis

We used AOT products from two satellite instruments to ensure robust results: the Moderate Resolution Imaging Spectroradiometer (MODIS) on the Terra/Aqua satellites [34–37] and the Visible Infrared Imaging Radiometer Suite (VIIRS) instrument on the Suomi National Polar-orbiting Partnership (S-NPP) spacecraft [26]. The daily ground $PM_{2.5}$ measurements for the six cities were released by the Ministry of Environmental Protection of China (MEPC). Zheng *et al.* [38] provided detailed descriptions on techniques and methods for $PM_{2.5}$ source apportionment in China. The MODIS instruments have 36 visible, near-infrared, and infrared spectral bands between 415 and 14,235 nano-meters (nm) with different spatial resolutions of 0.25, 0.50, or 1 km [37]. Time series global aerosol data has been

produced using images taken by the MODIS (Terra and Aqua) instruments since the launch in 1999 and 2002 [34–36]. MODIS Level-2 AOT product of orbital-swath is available at both 3 km and 10 km spatial resolution [37]. In addition, MODIS Level-3 AOT product from the computation of Level-2 product in each 1 ° × 1 °grid cell is also available, but with a relative coarse spatial resolution of 110 km [39].

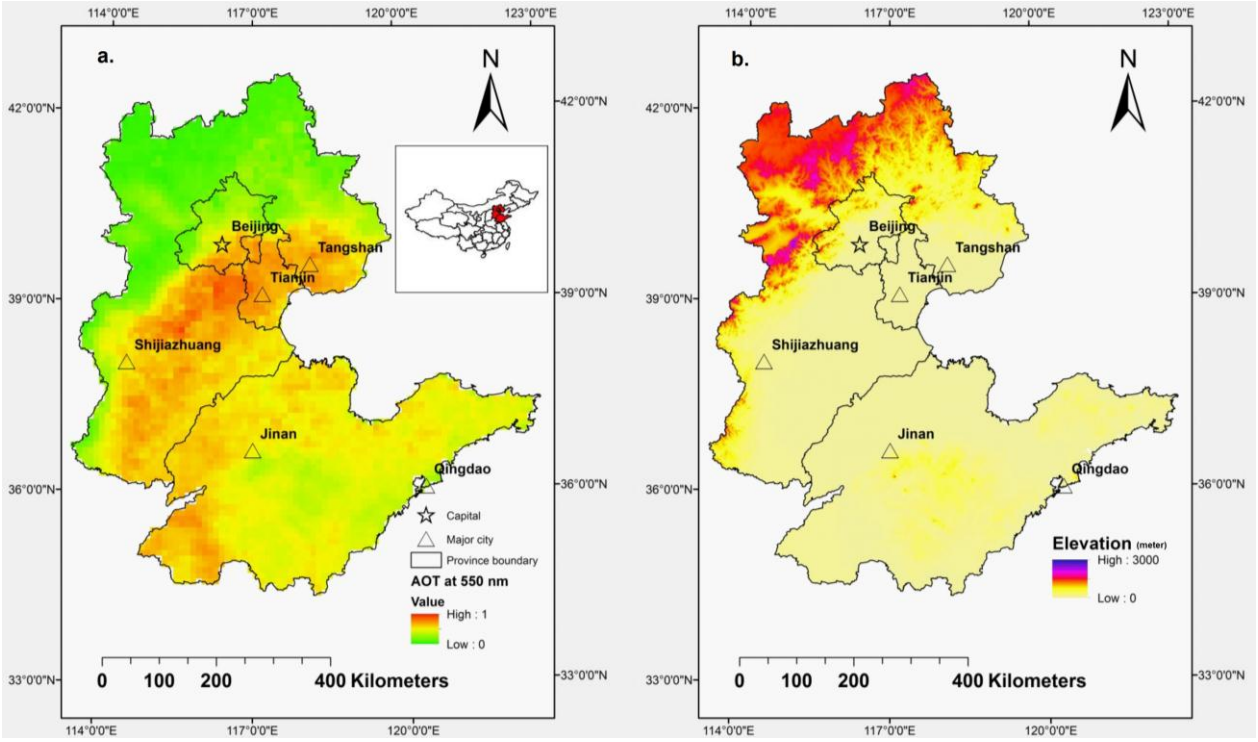

Figure 1. Study area (**a**) the mean MODIS Aerosol Optical Thickness (AOT) of 1–11 November 2002–2013; (**b**) Elevation. The city boundary of the six cities is provided by Data Center for Resources and Environmental Sciences, Chinese Academy of Sciences (DCRES, CAS). The Digital Elevation Model (DEM) was derived from the Shuttle Radar Topography Mission (SRTM).

Compared with MODIS, the VIIRS measure radiance in 22 spectral bands, spanning from 412 to 12,050 nm with different spatial resolutions of 0.375 and 0.75 km [26]. Since its launch in 2011, the AOT product has been produced using images taken by the VIIRS instruments. VIIRS AOT product is available at 6 km spatial resolution. The VIIRS aerosol algorithm was developed from the MODIS aerosol heritage, but significant differences exist between their final AOT products, mainly due to sensor differences and algorithm changes [26]. Detailed descriptions of the MODIS and VIIRS aerosol algorithms and their differences can be found in Kaufman *et al.* [34], Ginoux *et al.* [35], and Hsu *et al.* [36]. We used the Aqua MODIS and VIIRS AOT products, since they have the same overpass times for the study region (1:30 pm). All the MODIS and VIIRS AOT products were preprocessed in ENVI using MODIS Conversion Toolkit (MCTK) and VIIRS Conversion Toolkit (VCTK).

Missing data in the satellite AOT products is a consistent feature. It is either because the cloud calculation algorithm mistakenly masks dense smoke as cloud, or the AOT algorithm screens very high AOT values [39,40]. We found that the missing data issue was more severe for the MODIS AOT product at 3 km than at 10 km, within the study area during the 2014 Beijing APEC Meetings [37]. As a result,

we chose the MODIS AOT product at 10 km and the VIIRS AOT product at 6 km, using the 550 nm channel, to explore the aerosol loading patterns in Beijing and its five neighboring large cities.

To compare the performances of MODIS and VIIRS satellite instruments, we first extracted and averaged pixel values of MODIS and VIIRS products within the boundary of each city from 18 October 2014 to 30 November 2014. The six cities (*i.e.*, Beijing, Tianjin, Shijiazhuang, Tangshan, Jinan, and Qingdao) have 164, 118, 138, 128, 78, and 108 pixels, respectively. We firstly calculated the Spearman correlations [41] between daily mean AOT and corresponding ground-based $PM_{2.5}$ measurement for MODIS and VIIRS, respectively. Then, based on the 13-year (2002–2014) MODIS observations, we calculated standardized values (Z-scores) of mean AOT of the APEC period (1–11 November 2014) in six cities (Equation (1)).

$$z = \frac{X - \mu}{\sigma} \quad (1)$$

where X is the raw value, μ is the mean of AOT values of 1–11 November 2014, and σ is the standard deviation. These standardized values can be used for directly comparing AOT values in different years and locations, and emphasize extreme values [42]. Prior to the standardized values calculation in each city, we performed an additional log10 transformation on the period mean AOT to normalize the skewed distribution [42]. Finally, Spearman correlations in AOT Z-scores for 2002–2012 between Beijing and other five cities were calculated. In order to quantitatively analyze the effects of stringent emission control measures, mean AOT values were also calculated for three periods: pre-APEC (18–31 October), APEC (1–11 November), and post-APEC (12–30 November) in 2002–2014, respectively.

3. Results

Figure 2 shows the daily $PM_{2.5}$ and satellite-retrieved AOT measurements, from both MODIS and VIIRS instruments from 18 October to 30 November, 2014 for the six cities. Though having some anti-correlations, the mean AOT values for the six cities generally followed the ground $PM_{2.5}$ trends (Figure 1), suggesting that AOT data can generally reflect the near surface $PM_{2.5}$ concentration, which is indicative of air pollution levels [20]. Both daily $PM_{2.5}$ and AOT measurements can characterize the effects of emission control measures during the APEC period on the local air quality: for example, the peak values of $PM_{2.5}$ in Beijing were around 100 $\mu g \cdot m^{-3}$ during the APEC period; however, during the pre- and post-APEC periods, the peak values were up to 290 $\mu g \cdot m^{-3}$. Following the general $PM_{2.5}$ trend, the mean AOT for the six cities peaked around 0.49 and 2.84 during the APEC period and the pre- and post-APEC periods, respectively. In addition, Beijing, Tianjin, Shijiazhuang, and Tangshan had similar temporal variations in $PM_{2.5}$ and AOT values, compared with Jinan and especially Qingdao.

The linear correlation coefficients (R) (R = 0.55 for VIIRS and R = 0.66 for MODIS) confirmed the correlation between AOT and ground $PM_{2.5}$ (Figure 3a,b), although MODIS and especially VIIRS data tend to underestimate very high $PM_{2.5}$ mass (Figures 2 and 3a,b). During 19–21 November, despite the high peak value of ground $PM_{2.5}$ concentration (228 $\mu g \cdot m^{-3}$) in Beijing, the peak values of MODIS and VIIRS AOT (0.61 and 0.29 respectively) were relatively low; but they still followed the $PM_{2.5}$ trend. In addition, the missing data issue, as a consistent feature of AOT products, was more severe for MODIS (number of days with valid mean AOT values for all the six cities, N = 172) than for VIIRS (N = 211)

within the study area during the study period. However, a strong correlation existed between MODIS and VIIRS AOT values, based on valid daily measurements for both MODIS and VIIRS (R = 0.84; Figure 3c).

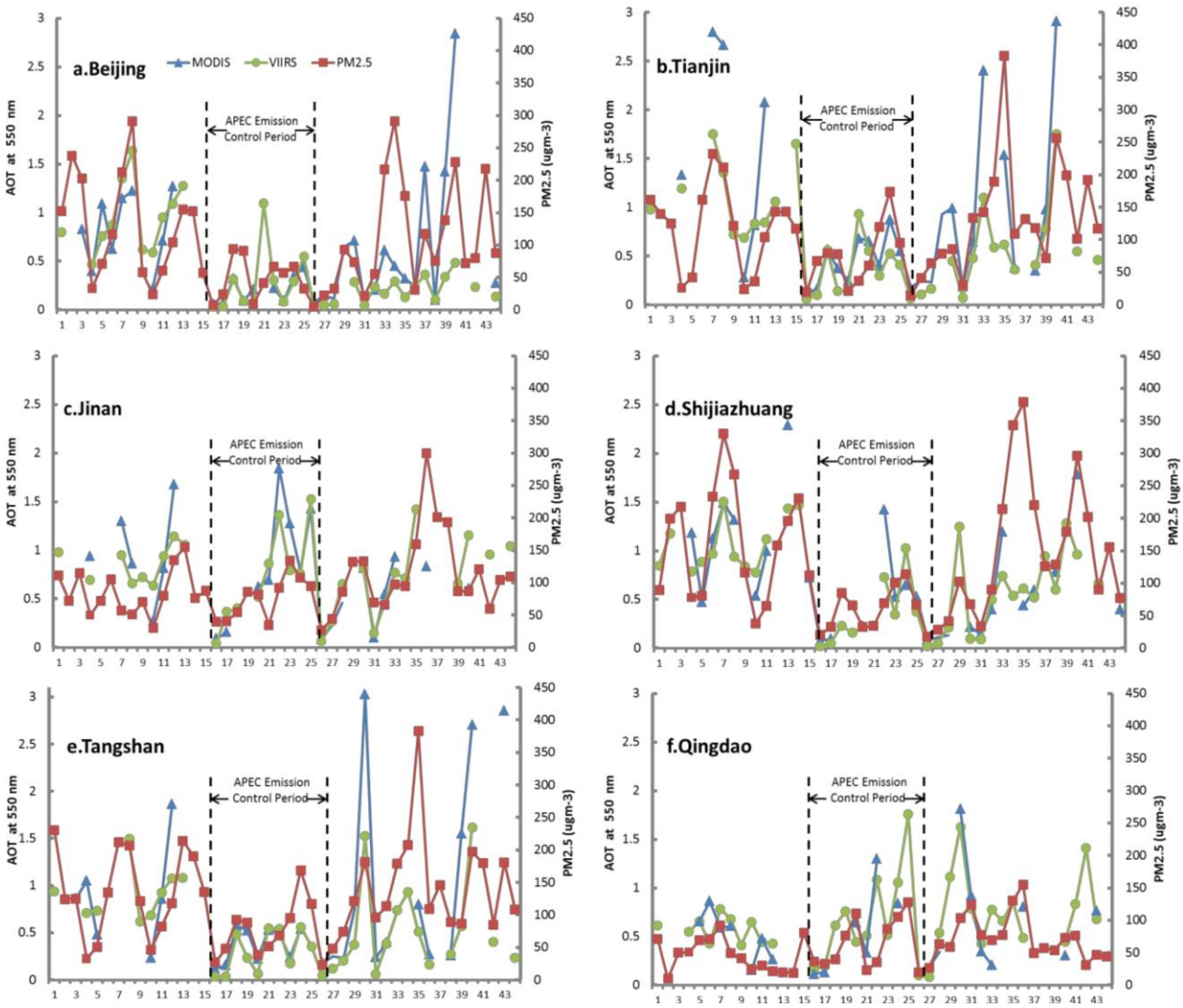

Figure 2. Daily satellite-retrieved mean AOT and ground $PM_{2.5}$ during three periods in six cities: pre-APEC (18–31 October, No. 1–14), APEC (1–11 November, No. 15–25), and post-APEC (12–30 November, No. 26–44) in 2014; No.1 on the x-axis denotes 18 October and so on; (**a**) Beijing, (**b**) Tianjin, (**c**) Shijiazhuang, (**d**) Tangshan, (**e**) Jinan, (**f**) Qingdao.

Figure 4 plots the aerosol loading during the APEC period and change in aerosol pollutants (1–11 November, 2002–2013 minus 1–11 November 2014), compared with the historical record (2002–2013), in terms of MODIS AOT value. Mean AOT value of Qingdao was lowest (0.33) during the APEC period (Figure 4a), among the six cities under study, e.g., 0.43 of Beijing, 0.45 of Tianjin, 0.39 of Shijiazhuang, 0.59 of Jinan, 0.35 of Tangshan. Although a portion of areas in southern Hebei and northern Shandong province showed increased AOT values, AOT values of northern Beijing (*i.e.*, Beijing's urban central areas) and its surroundings in Hebei province (approximately from Shijiazhuang to Tangshan) indicated an apparent spatial pattern of improved air quality during the APEC period (Figure 4b), compared with mean AOT values of the corresponding period of 2002–2013 (Figure 1a). The spatial heterogeneity in aerosol loading within Beijing was large during the APEC period, likely because the southern mountain

areas of Beijing usually had better air quality, compared with its northern urban central areas (Figure 1). As a result, Tangshan and Shijiazhuang—two cities in Hebei province—underwent the two largest decreases in AOT values (0.36 and 0.33 respectively). Mean AOT values in Beijing, Tianjin, and Qingdao decreased 0.11, 0.24, and 0.17, respectively; in contrast, mean AOT value of Jinan slightly increased 0.04.

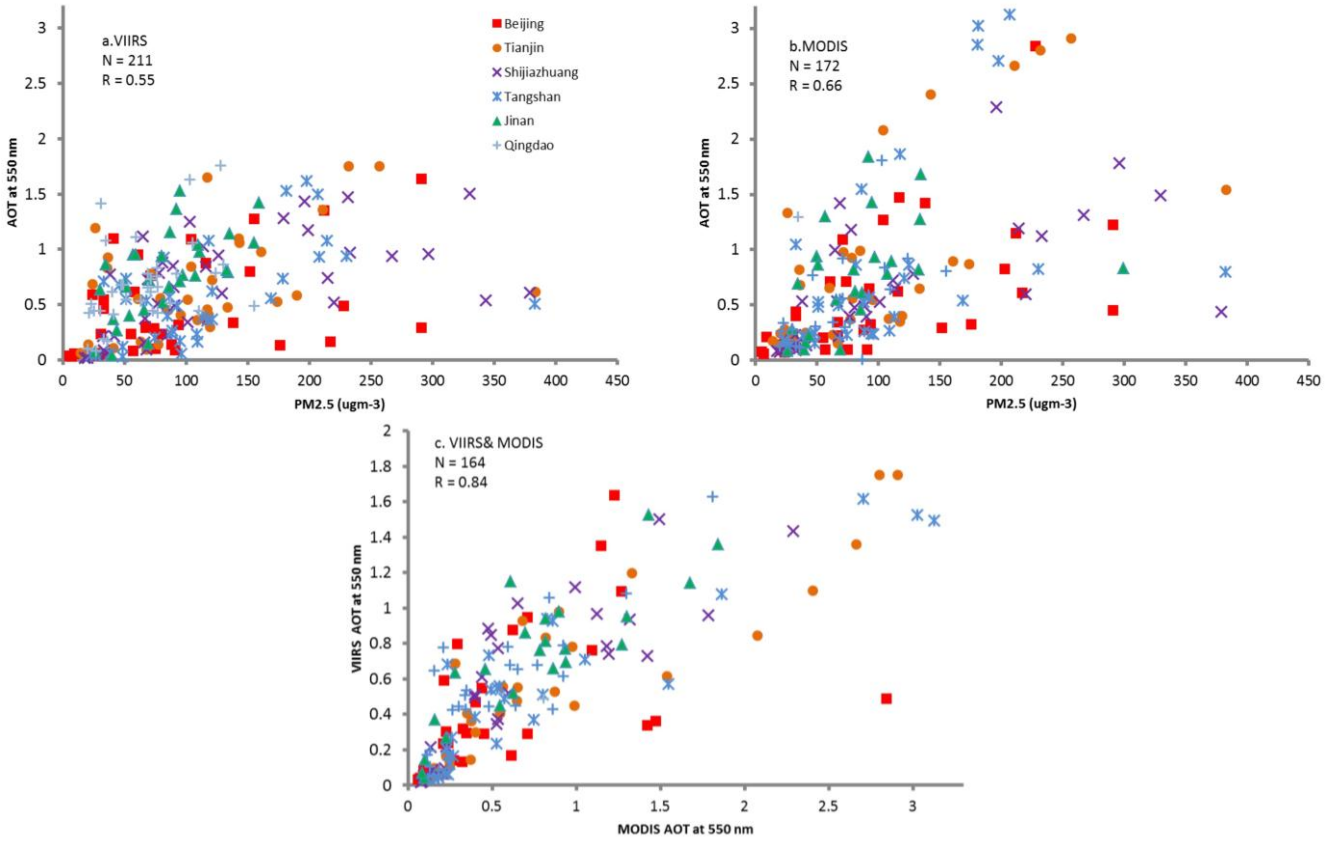

Figure 3. Scatter plots of mean AOT and ground $PM_{2.5}$ (18 October–30 November, 2014) for the six cities (**a**) VIIRS AOT and ground $PM_{2.5}$; (**b**) MODIS AOT and ground $PM_{2.5}$; (**c**) VIIRS AOT and MODIS AOT.

Figure 5 plots the change of mean MODIS AOT values during the pre-APEC (18–31 October), APEC (1–11 November), and post-APEC (12–30 November) periods from 2002 to 2014 annually in six cities. The temporal variation in AOT values of the three periods was hard to predict; nevertheless, consistent with Figure 2, the 2014 mean AOT values of the APEC period was less than that of both the pre-APEC and post-APEC period for all six cities. The largest difference in mean AOT values between the APEC period and other two periods was 1.56 of Tianjin, then 0.95 of Tangshan, 0.68 of Beijing, 0.61 of Shijiazhuang, 0.20 of Qingdao, and 0.05 of Jinan. Consistent with Figures 2 and 4, this phenomenon indicated the effectiveness of emission control measures, and that spatial heterogeneity in the improvement of air quality during the APEC period was apparent on the Northern China Plain.

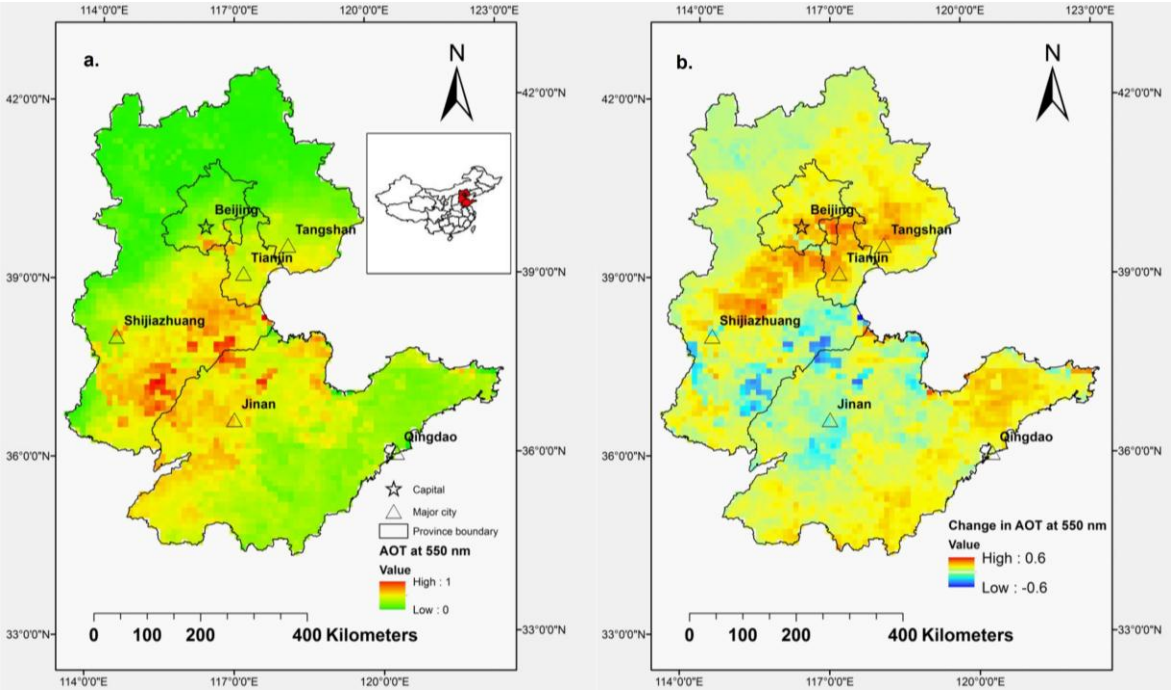

Figure 4. (**a**) MODIS mean AOT of 1–11 November 2014 (APEC blue period); (**b**) change in mean MODIS AOT values (1–11 November 2002–2013 minus 1–11 November 2014; positive values indicate increased air quality relative to historical mean; negative values indicate the opposite trend).

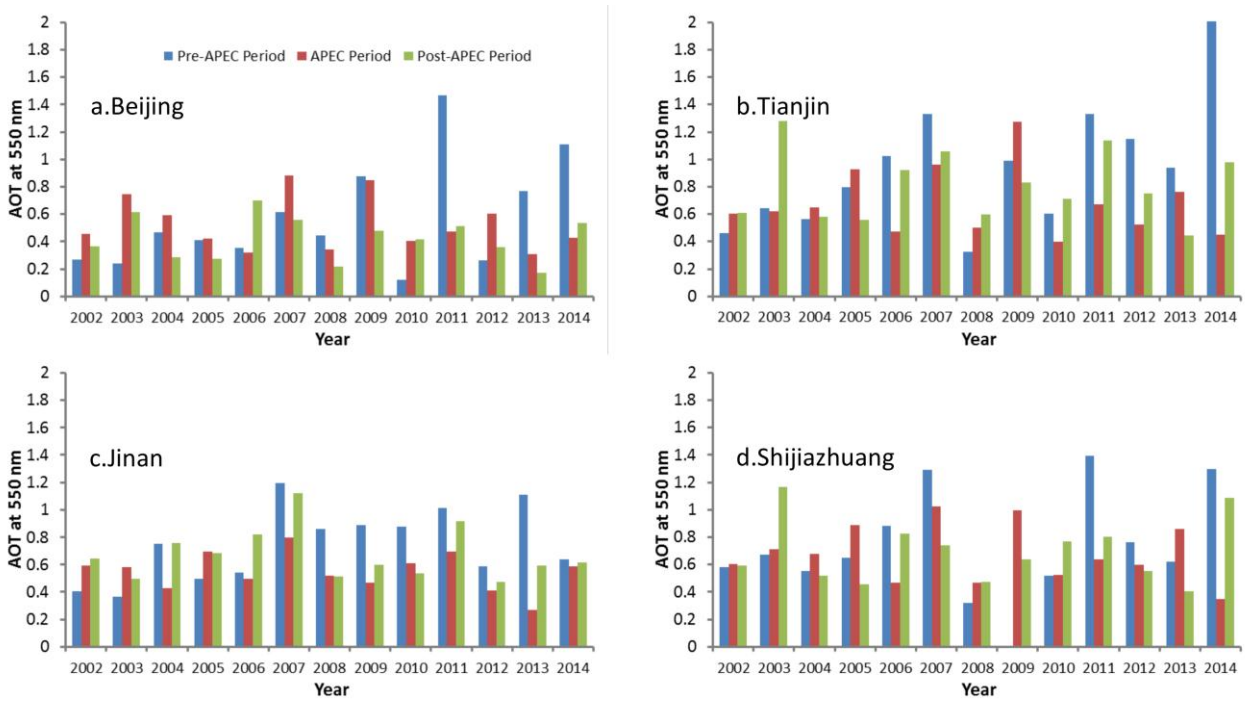

Figure 5. *Cont.*

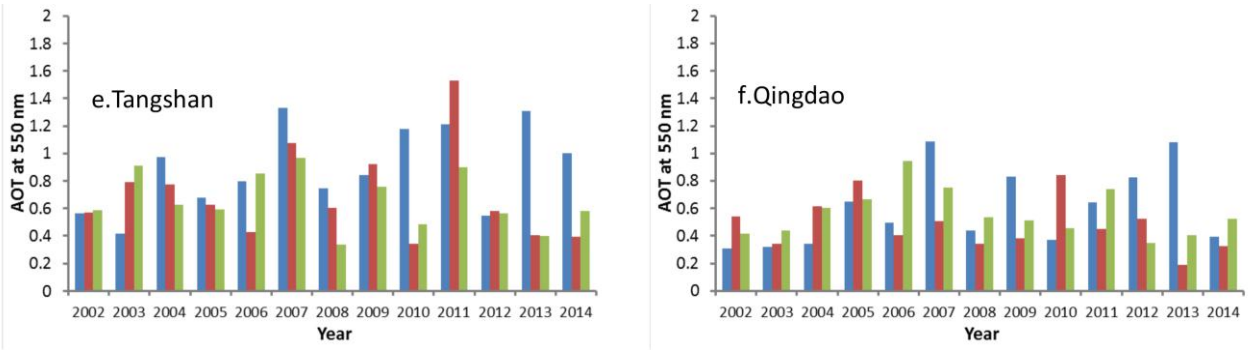

Figure 5. Mean AOT value before, during, and after APEC period from 2002 to 2014 (**a**) Beijing, (**b**) Tianjin (**c**) Jinan, (**d**) Shijiazhuang, (**e**) Tangshan, (**f**) Qingdao.

According to the news report [43], two stagnant atmospheric condition periods (around 9 November 2014 and 26 November 2014), reflecting unfavorable meteorological conditions for air quality [19], occurred during APEC and post-APEC period in Beijing. However, air quality was significantly different during these two periods (Figures 2 and 6). Specifically, on 9 November 2014, $PM_{2.5}$ level in Beijing (57 $\mu g \cdot m^{-3}$) was classified as moderate (Table 1, Figure 2); nevertheless, heavy pollution (228 $\mu g \cdot m^{-3}$) was monitored on 26 November 2014 (Table 1, Figure 2). Accordingly, AOT values of Beijing (0.09 for MODIS; 0.08 for VIIRS) and its surrounding areas (e.g., Tianjin, Tangshan, and Shijiazhuang) were much lower on 9 November 2014 than on 26 November 2014 (2.84 for MODIS, 0.49 for VIIRS; Figures 2 and 6). In contrast, the $PM_{2.5}$ in Jinan on these two dates demonstrated an opposite trend: the $PM_{2.5}$ level (134 $\mu g \cdot m^{-3}$) in Jinan was classified as minor pollution on 9 November 2014 and moderate on 26 November 2014 (87 $\mu g \cdot m^{-3}$; Table 1, Figure 2). Qingdao—the only city without stringent emission control measures among the six cities—just had a slight difference in $PM_{2.5}$ between these two dates (87 $\mu g \cdot m^{-3}$ and 73 $\mu g \cdot m^{-3}$, respectively; Table 1, Figure 2). AOT values of Jinan and Qingdao were also generally consistent with the corresponding values of $PM_{2.5}$, except the VIIRS AOT values of Jinan (Figures 2 and 6).

Table 1. Twenty-four hourly mean $PM_{2.5}$ ($\mu g \cdot m^{-3}$) and its corresponding Air Quality Index (AQI) and Air Quality Category (AQC) by MEPC.

	$PM_{2.5}$ ($\mu g \cdot m^{-3}$)					
	0–35	**36–75**	**76–115**	**116–150**	**151–250**	**>251**
AQI	0–50	51–100	101–150	151–200	201–300	>300
AQC	Good	Moderate	Minor pollution	Medium pollution	Heavy pollution	Very heavy pollution

Sea level pressure and surface wind plots, derived from ground-based meteorological data of NOAA's National Climatic Data Center (NCDC), show that stagnant atmospheric conditions persisted on 9 November 2014 and 26 November 2014 (Figure 7). The average surface wind speed was low (<3 m/s), and the majority of the North China Plain was controlled by a high pressure system on both days. The low wind speed is one key factor leading to poor air quality and low visibility in Beijing [44]. However, back trajectory calculations [45] show the regional circulation pattern was different on these two dates (Figure A1). It was a northwest wind on 9 November 2014, and the surface air mass was transported from the clean free troposphere. In contrast, the wind was from south of Beijing on 26 November and

the air mass was circulated within the boundary layer on the North China Plain. The mixing of agricultural, industrial, and urban emissions during this process especially favors accumulation of PM pollution.

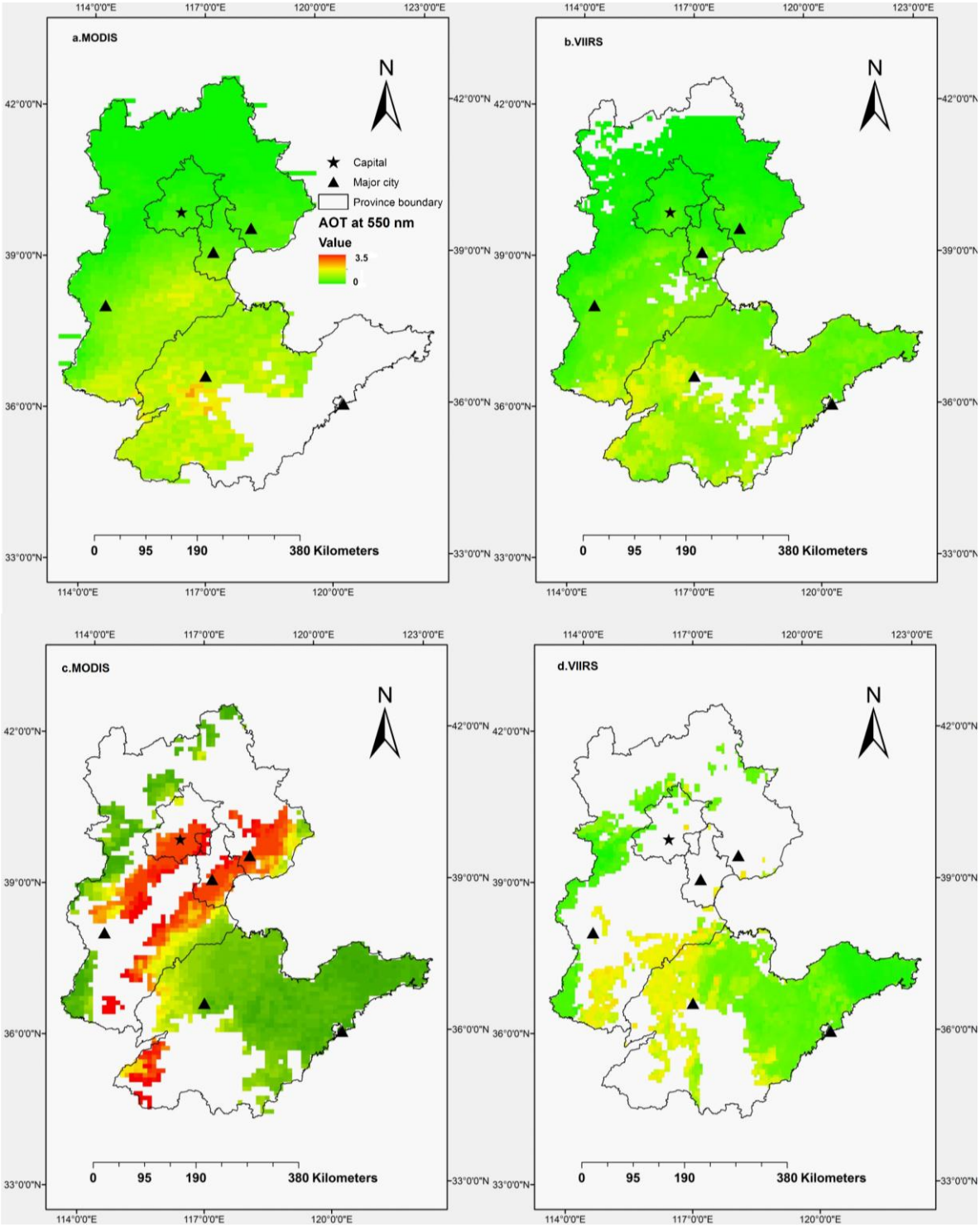

Figure 6. Satellite-retrieved AOT during and after the 2014 Beijing APEC Meetings in the study area. (**a**,**b**). 9 November 2014 (**c**,**d**). 26 November 2014 (both dates have stagnant atmospheric conditions).

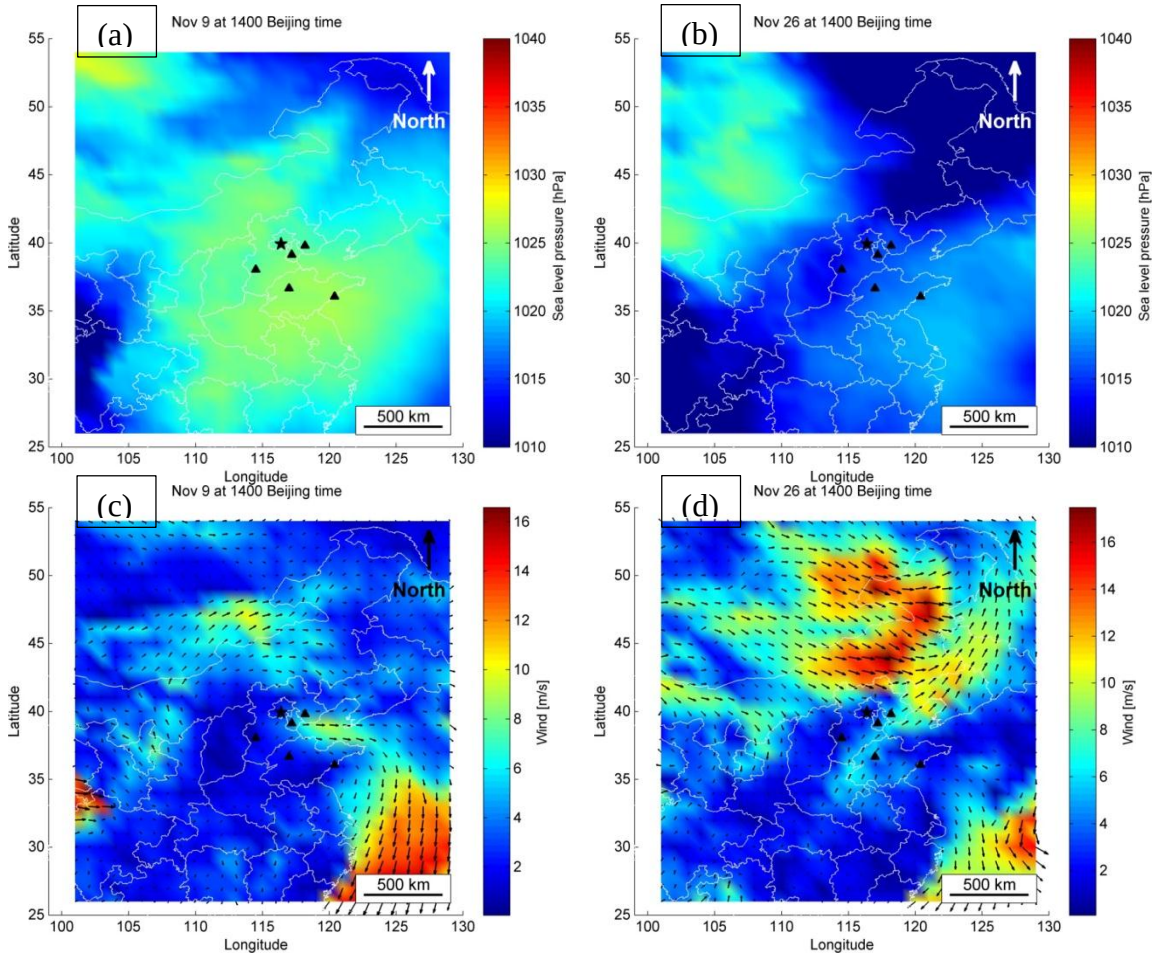

Figure 7. Sea level pressure plots ((**a**) 9 November 2014 and (**b**) 26 November 2014) and surface wind plots ((**c**) 9 November 2014 and (**d**) 26 November 2014) derived from NCDC observations.

Z-scores in Beijing, Tianjin, Shijiazhuang, Tangshan, and Qingdao during the 2014 APEC Meetings was relatively low to historical mean, suggesting the air quality of the 2014 APEC period was higher than the average of the corresponding period of 2002–2013 (Figure 8). However, consistent with Figure 4b, mean AOT value of Jinan is below the historical mean. Temporal variations in mean AOT values of the six cities were very high; nevertheless, strong temporal correlations in mean AOT still existed between Beijing and Tianjin (0.79), Shijiazhuang (0.82), Tangshan (0.88), with the exception of Jinan (0.07) and Qingdao (0.32) (Figure 8, Table 2).

Table 2. Spearman correlation of Z-score of mean MODIS AOT values of the APEC period (1–11 November) between Beijing and Tianjin, Shijiazhuang, Tangshan, Jinan, and Qingdao.

City	Tianjin	Shijiazhuang	Tangshan	Jinan	Qingdao
Spearman Correlation	0.79	0.82	0.88	0.07	0.32

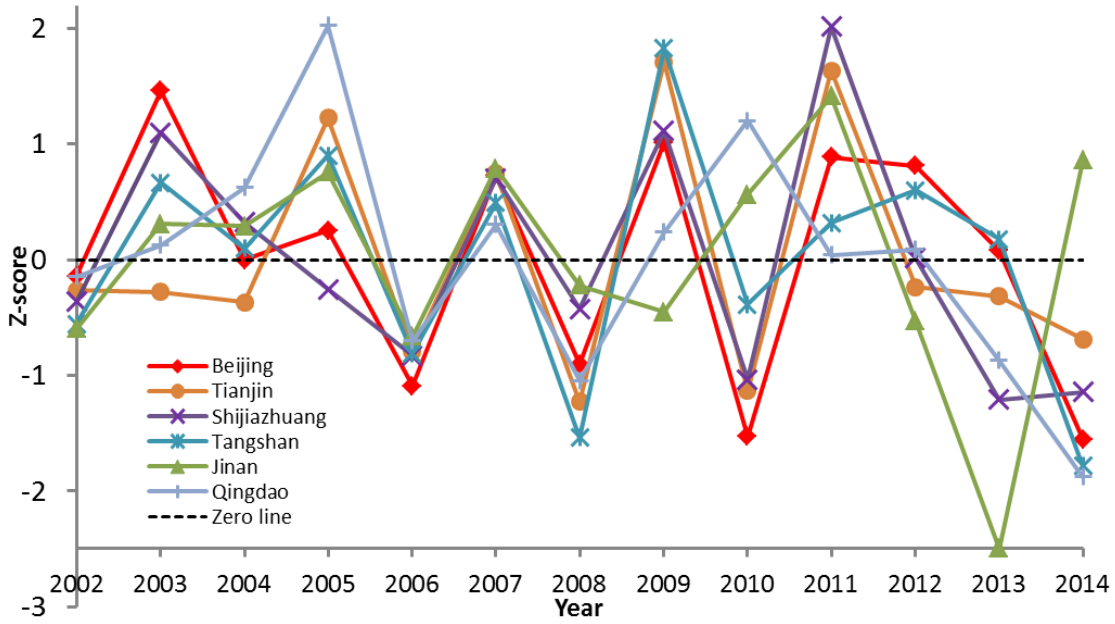

Figure 8. Z-score of mean MODIS AOT values during the APEC period (1–11 November) in six cities for the past 13 years (2012–2014).

4. Discussion

By examining the ground $PM_{2.5}$ measurements and remote sensing AOT products, spatial heterogeneity of change in aerosol pollutants relative to historical mean was apparent during the APEC period on the Northern China Plain (Figure 4b): southern Beijing (*i.e.*, Beijing's urban areas) and its surroundings (e.g., Tangshan, Tianjin and Shijiazhuang) experienced dramatic improvement in air quality during the 2014 Beijing APEC Meetings, compared with the corresponding period of 2002–2014; northern Shandong (e.g., Jinan) and southern Hebei areas had relatively higher AOT values during the APEC period, compared with historical mean. However, different from the similar analysis at the province scale [3], the quantitative analysis of the changes of AOT in Jinan still indicated the APEC period had the best air quality during the three periods (Figure 5). Qingdao also had a similar phenomenon (Figure 5). These results suggest the effectiveness of stringent emission control measures during the 2014 Beijing APEC Meetings and the effects of regional transport on air quality on the Northern China Plain [3,18,19]. In addition to geographic locations, emission intensity, and strictness of emission control measures as suggested by Huang *et al.* [3], the back trajectory analysis in this study indicated that regional transport pattern might play an important role in the spatial heterogeneity of change in aerosol pollutants relative to historical mean and contribute to the APEC Blue in Beijing (Figure 6, Figure A1): the wind was northwest, when stagnant atmospheric condition persisted during the APEC period; in contrast, wind was south, when another stagnant atmospheric condition persisted during the post-APEC period. The difference in regional transport pattern might also explain why the air quality in Jinan on 9 November 2014 was worse than on 26 November 2014, although having emission control measures. Probably because of the strong effects of regional transport pattern on the short time air quality on the Northern China Plain, Z-score of mean AOT values of the study period in six cities oscillated for the past 13 years (Figure 8).

Using a spatial correlation analysis method based on remote sensing product during the study period in 2011–2013, Huang *et al.* [3] identified that the potential emission source regions, impacting air quality of Beijing, included most areas of Hebei, Tianjin, Shandong, and Shanxi (not included in this study). Based on a finer spatial resolution remote sensing product during the study period in 2002–2013, the analysis in our study further indicated that the potential emission source regions strongly impacting air quality of Beijing were confined within central and southern Hebei as well as northern and southwestern Shandong, in correspondence with the spatial pattern of DEM of the study region (Figure 1). One explanation is that the human population density and the abundance of urban development tend to be high at lower elevations near rivers and sea coasts [46], so more intense emissions of aerosol pollutants are expected at lower elevations of Northern China Plain where several major rivers (e.g., Yellow River) run into the sea. Another explanation is that topography can strongly affect the regional transport pattern [47]. However, most important of all, with the roaring development of China's industry for the past three decades, coal consumption in China accounted for 50% of the world's total coal consumption by 2012, as high as 1.63 billion tons of oil equivalent [48]. Coal-intensive industries (e.g., iron and steel) are concentrated in northern China including Shandong and especially Hebei [49]. As a result, during the first half year of 2013, seven of the top ten polluted cities in China were within Hebei, and what is more, three cities in southern Hebei including Shijiazhuang were the top three polluted cities [17]. The result of following temporal correlation analysis of mean AOT values between Beijing and its five neighboring large cities for the past thirteen years (2002–2014) was consistent with the spatial pattern of the mean AOT values of the study period in 2002–2013: strong temporal correlations were found between Beijing and Tianjin (R = 0.79), Shijiazhuang (R = 0.82), and Tangshan (R = 0.88). Qingdao, far away from Beijing, had a weak temporal correlation of 0.32. The very weak temporal correlation of Jinan (R = 0.07) may be because it is downwind of central and southern Hebei, where there are major emission source regions on the North China Plain, in contrast to Beijing.

We used ground $PM_{2.5}$ measurement, VIIRS AOT product, and MODIS AOT product in particular to evaluate the impact of emission control measures on aerosol pollutants during the three APEC-related periods. Only moderate correlations (0.66 for MODIS and 0.55 for VIIRS) were found between remote sensing AOT products and $PM_{2.5}$ ground measurement in this study, but still comparable to the previous similar study (R = 0.70) [20]. The disparity between remote sensing AOT products and ground $PM_{2.5}$ measurement in this study can be explained by the fact that the ground $PM_{2.5}$ measurement represents the air quality of daily average, but remote sensing products show a snapshot of aerosol pollutants of satellite overpass time. An uncertainty of MODIS optical retrievals within $\Delta\tau = \pm 0.05 \pm 0.15\tau$ over land was reported after the comprehensive validation of MODIS AOT product [50–53]. Consistent with the preliminary validation of VIIRS AOT product showing the 71% of optical retrievals over land falling within the expected uncertainty range of MODIS [54], a strong correlation was found between MODIS and VIIRS AOT product (Figure 3c). These validation results show that the remote sensing AOT products can be used for quantitative scientific investigations and monitoring of aerosol loading and distribution [3,54].

The health impact of aerosol loading is mostly related to $PM_{2.5}$ values at the surface. We demonstrated that both MODIS and VIIRS captured the variation in aerosol loading during the three APEC-related periods, as evidenced by surface $PM_{2.5}$ measurements in six central cities on the North China Plain. Remote sensing AOT products can be used to supplement ground measurement for monitoring air quality and estimating surface aerosol loading over a large spatial-temporal domain, considering the usually sparsity of surface aerosol monitoring sites. However, our study also indicated the potential disparity that existed between current MODIS and VIIRS AOT product and ground measurement, so further explorations on the relationship between $PM_{2.5}$ and satellite derived aerosol properties are still needed. With the deployment of new remote sensing and *in situ* sensors for mapping aerosol distribution, such as Lidar, more development can be expected in remote sensing of aerosol loading in the future [55].

5. Conclusions

In conclusion, consistent with the similar air pollution studies [3,15,16,32] in Beijing, our results suggested that the APEC Blue was a regional phenomenon for a temporary period and it was in all likelihood caused by the combined effects of stringent emission control measures and relative favorable regional transport pattern during the 2014 Beijing APEC Meetings. However, a long-term improvement of air quality in Beijing is still challenging and joint efforts of the whole region are needed.

Acknowledgments

This study was funded by the grant of Beijing Municipal Bureau of Landscape and Forestry "Monitor and Evaluation on the Development of the Beijing-Hebei Protection Forests for Ecological Service and Headwater Conservation" (2013HXFWJGXY010). The authors would like to thank the data providers for this study. The MODIS data for this paper is available at NASA's Atmosphere Archive and Distribution System (Data set: MODIS04). The VIIRS data for this paper is available at NOAA's Comprehensive Large Array Data Stewardship System (Data set: VIIRS_EDR). The ground $PM_{2.5}$ data for this paper is available at a website called Tianqihoubao (http://www.tianqihoubao.com/). The SRTM DEM is downloaded from the NASA Jet Propulsion Laboratory. MCTK and VCTK are developed by Devin White and downloaded from GitHub. The authors would also like to thank Weishu Gong and Cheryl Nichols for proofreading the manuscript and providing suggestions.

Author Contributions

Ran Meng, Feng Zhao, Chengquan Huang, and Jianying Yang conceived the idea and designed the methodology; Ran Meng, Feng Zhao, Sun Kang, and Rui Zhang performed the data analysis; Ran Meng, Feng Zhao, and Sun Kang prepared the manuscript; Ran Meng, Feng Zhao, Chengquan Huang, Jianying Yang, and Sun Kang contributed to the discussion.

Conflicts of Interest

The authors declare no conflict of interest.

Appendix

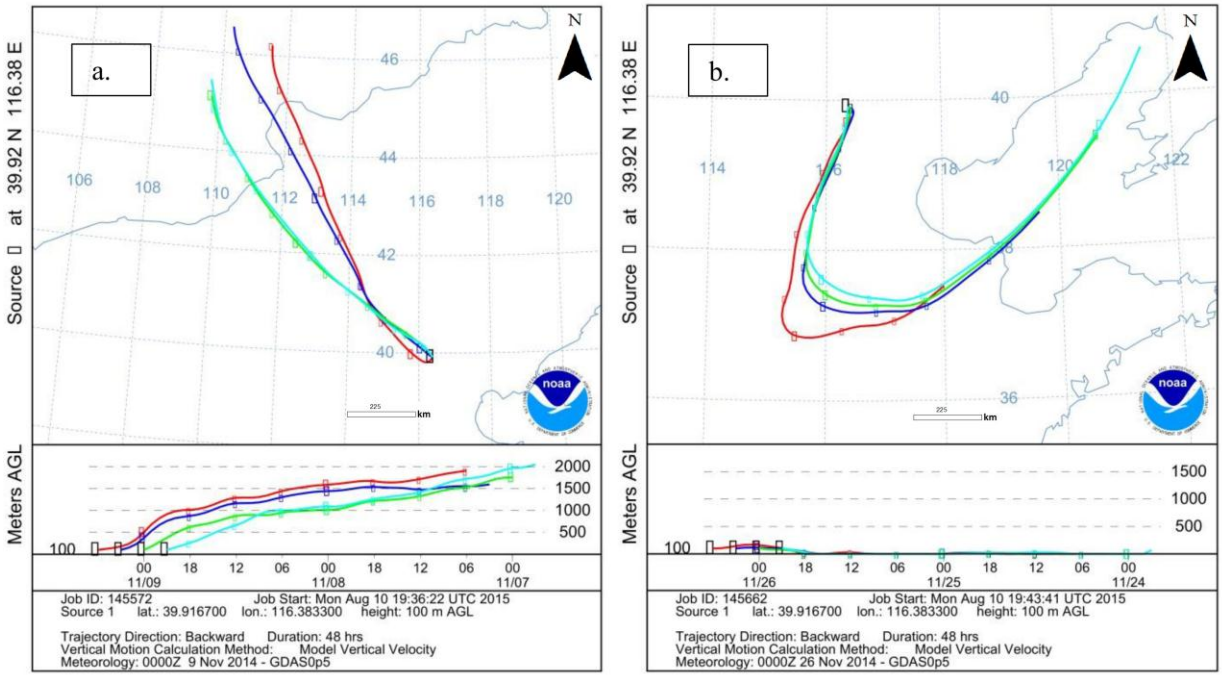

Figure A1. Back trajectory analysis using Beijing as the source; (**a**). 9 November 2014; (**b**). 26 November 2014.

Reference

1. Li, M.; Zhang, L. Haze in China: Current and future challenges. *Environ. Pollut*. **2014**, *189*, 85–90.
2. Tang, D.; Li, T.Y.; Chow, J.C.; Kulkarni, S.U.; Watson, J.G.; Ho, S.S.H.; Quan, Z.Y.; Qu, L.R.; Perera, F. Air pollution effects on fetal and child development: A cohort comparison in China. *Environ. Pollut*. **2014**, *185*, 90–95.
3. Huang, K.; Zhang, X.; Lin, Y. The "APEC Blue" phenomenon: Regional emission control effects observed from space. *Atmos. Res.* **2015**, *164*, 65–75.
4. Dexter R. Bloomberg: Beijing Aims to Reduce Hazardous Smog Ahead of APEC. Available online: http://www.bloomberg.com/bw/articles/2014–10–10/beijing-aims-to-reduce-hazardous-smog-ahead-of-apec (accessed on 18 March 2015).
5. Tang K. Thanks to APEC, Beijing Gets Another "Golden Week". Available online: http://www.cnbc.com/id/102153174/ (Accessed on 18 March 2015).
6. Zheng J. Beijing to Keep the Lid on Air Pollution for APEC. Available online: http://www.chinadaily.com.cn/china/2014–10/10/content_18714550.htm (accessed on 18 March 2015).
7. Ramanathan, V.; Crutzen, P.; Kiehl, J.; Rosenfeld, D. Aerosols, climate, and the hydrological cycle. *Science* **2001**, *294*, 2119–2124.
8. Gustafsson, Ö.; Kruså, M.; Zencak, Z.; Sheesley, R.J.; Granat, L.; Engström, E.; Praveen, P.S.; Rao, P.S.P.; Leck, C.; Rodhe, H. Brown clouds over South Asia: Biomass or fossil fuel combustion? *Science* **2009**, *323*, 495–498.

9. Tao, M.; Chen, L.; Su, L.; Tao, J. Satellite observation of regional haze pollution over the North China Plain. *J. Geophys. Res.: Atmos.* **2012**, *117*, D12.
10. Zhang, Z.; Zhang, X.; Gong, D.; Quan, W.; Zhao, X.; Ma, Z.; Kim, S.-J. Evolution of surface O_3 and $PM_{2.5}$ concentrations and their relationships with meteorological conditions over the last decade in Beijing. *Atmos. Environ.* **2015**, *108*, 67–75.
11. Burnett, R.T.; Pope, C.A.; Ezzati, M.; Olives, C.; Lim, S.S.; Mehta, S.; Shin, H.H.; Singh, G.; Hubbell, B.; Brauer, M. An integrated risk function for estimating the global burden of disease attributable to ambient fine particulate matter exposure. *Environ. Health Perspect.* **2014**, *122*, 397–403.
12. Laden, F.; Neas, L.M.; Dockery, D.W.; Schwartz, J. Association of fine particulate matter from different sources with daily mortality in six US cities. *Environ. Health Perspect.* **2000**, *108*, 941–947.
13. Jia, Y.; Stone, D.; Wang, W.; Schrlau, J.; Tao, S.; Massey Simonich, S.L. Estimated reduction in cancer risk due to pah exposures if source control measures during the 2008 Beijing olympics were sustained. *Environ. Health Perspect.* **2011**, *119*, 815–820.
14. Worden, H.M.; Cheng, Y.; Pfister, G.; Carmichael, G.R.; Zhang, Q.; Streets, D.G.; Deeter, M.; Edwards, D.P.; Gille, J.C.; Worden, J.R. Satellite-based estimates of reduced CO and CO_2 emissions due to traffic restrictions during the 2008 Beijing Olympics. *Geophys. Res. Lett.* **2012**, *39*, doi:10.1029/2012GL052395.
15. Streets, D.G.; Fu, J.S.; Jang, C.J.; Hao, J.; He, K.; Tang, X.; Zhang, Y.; Wang, Z.; Li, Z.; Zhang, Q. Air quality during the 2008 Beijing Olympic Games. *Atmos. Environ.* **2007**, *41*, 480–492.
16. Mijling, B.; van der A, R.J.; Boersma, K.F.; Van Roozendael, M.; De Smedt, I.; Kelder, H.M. Reductions of NO_2 detected from space during the 2008 Beijing Olympic Games. *Geophys. Res. Lett.* **2009**, *36*, L13801.
17. Wang, L.T.; Wei, Z.; Yang, J.; Zhang, Y.; Zhang, F.F.; Su, J.; Meng, C.C.; Zhang, Q. The 2013 severe haze over southern Hebei, China: Model evaluation, source apportionment, and policy implications. *Atmos. Chem. Phys.* **2013**, *14*, 3151–3173.
18. Zhang, J.K.; Wang, L.L.; Wang, Y.H.; Wang, Y.S. Submicron aerosols during the Beijing Asia-Pacific Economic Cooperation Conference in 2014. *Atmos. Environ.* **2015**, in press.
19. Yang, H.; Chen, J.; Wen, J.; Tian, H.; Liu, X. Composition and sources of $PM_{2.5}$ around the heating periods of 2013 and 2014 in Beijing: Implications for efficient mitigation measures. *Atmos. Environ.* **2015**, in press.
20. Wang, J.; Christopher, S.A. Intercomparison between satellite-derived aerosol optical thickness and $PM_{2.5}$ mass: Implications for air quality studies. *Geophys. Res. Lett.* **2003**, *30*, doi:10.1029/2003GL018174.
21. van Donkelaar, A.; Martin, R.V.; Levy, R.C.; da Silva, A.M.; Krzyzanowski, M.; Chubarova, N.E.; Semutnikova, E.; Cohen, A.J. Satellite-Based estimates of ground-level fine particulate matter during extreme events: A case study of the Moscow fires in 2010. *Atmos. Environ.* **2011**, *45*, 6225–6232.
22. Mei, L.; Xue, Y.; de Leeuw, G.; Guang, J.; Wang, Y.; Li, Y.; Xu, H.; Yang, L.; Hou, T.; He, X., *et al.* Integration of remote sensing data and surface observations to estimate the impact of the Russian wildfires over Europe and Asia during August 2010. *Biogeosci. Discuss.* **2011**, *8*, 7741–7790.
23. Guo, Y.; Feng, N.; Christopher, S.A.; Kang, P.; Zhan, F.B.; Hong, S. Satellite remote sensing of fine particulate matter ($PM_{2.5}$) air quality over beijing using MODIS. *Int. J. Remote Sens.* **2014**, *35*, 6522–6544.

24. Dinoi, A.; Perrone, M.R.; Burlizzi, P. Application of MODIS products for air quality studies over southeastern Italy. *Remote Sens.* **2010**, *2*, 1767–1796.
25. Gao, J.; Zha, Y. Meteorological influence on predicting air pollution from MODIS-derived aerosol optical thickness: A case study in Nanjing, China. *Remote Sens.* **2010**, *2*, 2136–2147.
26. Jackson, J.M.; Liu, H.; Laszlo, I.; Kondragunta, S.; Remer, L.A.; Huang, J.; Huang, H.C. Suomi-NPP VIIRS aerosol algorithms and data products. *J. Geophys. Res.: Atmos.* **2013**, *118*, 12–673.
27. Pickering, K.E.; Wang, Y.; Tao, W.K.; Price, C.; Müller, J.F. Vertical distributions of lightning NO_X for use in regional and global chemical transport models. *J. Geophys. Res.: Atmos* **1998**, *103*, 31203–31216.
28. Parrington, M.; Palmer, P.I.; Henze, D.K.; Tarasick, D.W.; Hyer, E.J.; Owen, R.C.; Helmig, D.; Clerbaux, C.; Bowman, K.W.; Deeter, M.N. The influence of boreal biomass burning emissions on the distribution of tropospheric ozone over North America and the North Atlantic during 2010. *Atmos. Chem. Phys.* **2012**, *12*, 2077–2098.
29. Schutgens, N.; Nakata, M.; Nakajima, T. Estimating aerosol emissions by assimilating remote sensing observations into a global transport model. *Remote Sens.* **2012**, *4*, 3528–3543.
30. China, the State Council. Air Pollution Prevention And Control Action Plan. Avaliable online: http://www.gov.cn/zwgk/2013-09/12/content_2486773.htm (accessed on 9 November 2015). (In Chinese).
31. Guo, S.; Hu, M.; Zamora, M.L.; Peng, J.; Shang, D.; Zheng, J.; Du, Z.; Wu, Z.; Shao, M.; Zeng, L. Elucidating severe urban haze formation in china. *Proc. Natl. Acad. Sci. USA* **2014**, *111*, 17373–17378.
32. Li, P.; Yan, R.; Yu, S.; Wang, S.; Liu, W.; Bao, H. Reinstate regional transport of $PM_{2.5}$ as a major cause of severe haze in Beijing. *Proc. Natl. Acad. Sci. USA* **2015**, *112*, E2739–E2740.
33. Zhang, R.; Guo, S.; Zamora, M.L.; Hu, M. Reply to Li *et al.*: Insufficient evidence for the contribution of regional transport to severe haze formation in Beijing. *Proc. Natl. Acad. Sci. USA* **2015**, *112*, E2741.
34. Kaufman, Y.J.; Tanré, D.; Remer, L.A.; Vermote, E.F.; Chu, A.; Holben, B.N. Operational remote sensing of tropospheric aerosol over land from EOS moderate resolution imaging spectroradiometer. *J. Geophys. Res.: Atmos.* **1997**, *102*, 17051–17067.
35. Ginoux, P.; Garbuzov, D.; Hsu, N.C. Identification of anthropogenic and natural dust sources using moderate resolution imaging spectroradiometer (MODIS) deep blue level 2 data. *J. Geophys. Res.: Atmos.* **2010**, *115*, D5.
36. Hsu, N.C.; Tsay, S.-C.; King, M.D.; Herman, J.R. Aerosol properties over bright-reflecting source regions. *IEEE Trans. Geosci. Remote Sens.* **2004**, *42*, 557–569.
37. Livingston, J.M.; Redemann, J.; Shinozuka, Y.; Johnson, R.; Russell, P.B.; Zhang, Q.; Mattoo, S.; Remer, L.; Levy, R.; Munchak, L. Comparison of MODIS 3 km and 10 km resolution aerosol optical depth retrievals over land with airborne sunphotometer measurements during ARCTAS summer 2008. *Atmos. Chem. Phys.* **2014**, *14*, 2015–2038.
38. Zheng, M.; Zhang, Y.; Yan, C.; Zhu, X.; Schauer, J.J.; Zhang, Y. Review of $PM_{2.5}$ source apportionment methods in China. *ACTA Sci. Nat. Univ. Pekin.* **2014**, *50*, doi:10.13209/j.0479-8023.2014.068. (In Chinese).

39. Hubanks, P.; Platnick, S.; King, M.; Ridgway, B.; MODIS Atmosphere L3 Gridded Product Algorithm Theoretical Basis Document (ATBD) & Users Guide. Available online: https://modis-atmos.gsfc.nasa.gov/_docs/L3_ATBD_C6_2015_05_06.pdf (accessed on 9 November 2015).
40. Engel-Cox, J.A.; Holloman, C.H.; Coutant, B.W.; Hoff, R.M. Qualitative and quantitative evaluation of MODIS satellite sensor data for regional and urban scale air quality. *Atmos. Environ.* **2004**, *38*, 2495–2509.
41. Spearman, C. The proof and measurement of association between two things. *Am. J. Psychol.* **1904**, *15*, 72–101.
42. Meng, R.; Dennison, P.; Huang, C.; Moritz, M.; D'Antonio, C. Effects of fire severity and post-fire climate on short-term vegetation recovery of mixed-conifer and red fir forests in the Sierra Nevada Mountains of California. *Remote Sens. Environ.* **2015**, *171*, 311–325
43. Beijing-Youth-Daily. Persistent Faze Weather until the End of November in Beijing-Tianjing-Hebei Areas. Available online: http://epaper.Ynet.Com/html/2014–11/22/content_98052.Htm?Div=-1 (accessed on 18 March 2015). (In Chinese).
44. Wu, Z.; Hu, M.; Lin, P.; Liu, S.; Wehner, B.; Wiedensohler, A. Particle number size distribution in the urban atmosphere of Beijing, China. *Atmos. Environ.* **2008**, *42*, 7967–7980.
45. Draxler, R.R.; Rolph, G.D. Hysplit (Hybrid Single-Particle Lagrangian Integrated Trajectory) Model. Available online: http://www.arl.noaa.gov/ready/hysplit4.html (accessed on 9 November 2015).
46. Small, C.; Cohen, J.E. Continental physiography, climate, and the global distribution of human population. *Curr. Anthro.* **2004**, *45*, 269–277.
47. Meixner, F.X.; Eugster, W. Effects of landscape pattern and topography on emissions and transport. In *Integrating Hydrology, Ecosystem Dynamics, and Biogeochemistry in Complex Landscapes*. Wiley: New York, NY, USA, 1999; pp. 147–175.
48. Chen, Z.; Wang, J.N.; Ma, G.X.; Zhang, Y.S. China tackles the health effects of air pollution. *Lancet* **2013**, *382*, 1959–1960.
49. Hao, Y.; Zhang, Z.Y.; Liao, H.; Wei, Y.M. China's farewell to coal: A forecast of coal consumption through 2020. *Energy Policy* **2015**, *86*, 444–455.
50. Chu, D.A.; Kaufman, Y.J.; Ichoku, C.; Remer, L.A.; Tanré, D.; Holben, B.N. Validation of MODIS aerosol optical depth retrieval over land. *Geophys. Res. Lett.* **2002**, *29*, MOD2-1–MOD2-4.
51. Kahn, R.; Nelson, D.L.; Garay, M.J.; Levy, R.C.; Bull, M.; Diner, D.J.; Martonchik, J.V.; Paradise, S.R.; Hansen, E.G.; Remer, L. MISR aerosol product attributes and statistical comparisons with MODIS. *IEEE Trans. Geosci. Remote Sens.* **2009**, *47*, 4095–4114.
52. Levy, R.C.; Remer, L.A.; Kleidman, R.G.; Mattoo, S.; Ichoku, C.; Kahn, R.; Eck, T.F. Global evaluation of the collection 5 MODIS dark-target aerosol products over land. *Atmos. Chem. Phys.* **2010**, *10*, 10399–10420.
53. Remer, L.A.; Kaufman, Y.J.; Tanré, D.; Mattoo, S.; Chu, D.A.; Martins, J.V.; Li, R.R.; Ichoku, C.; Levy, R.C.; Kleidman, R.G. The MODIS aerosol algorithm, products, and validation. *J. Atmos. Sci.* **2005**, *62*, 947–973.

54. Liu, H.; Remer, L.A.; Huang, J.; Huang, H.C.; Kondragunta, S.; Laszlo, I.; Oo, M.; Jackson, J.M. Preliminary evaluation of S-NPP VIIRS aerosol optical thickness. *J. Geophys. Res.: Atmos.* **2014**, *119*, 3942–3962.
55. Chu, D.A.; Ferrare, R.; Szykman, J.; Lewis, J.; Scarino, A.; Hains, J.; Burton, S.; Chen, G.; Tsai, T.; Hostetler, C.; *et al.* Regional characteristics of the relationship between columnar AOD and surface $PM_{2.5}$: Application of lidar aerosol extinction profiles over Baltimore–Washington corridor during discover-AQ. *Atmos. Environ.* **2015**, *101*, 338–349.